Observation of efficient sub-Doppler cooling under a nonzero magnetic field in a moving optical lattice

Jung-Ryul Kim,[*] Kyeong Ock Chong,[†] Jinuk Kim, and Kyungwon An[‡]

Department of Physics and Astronomy & Institute of Applied Physics, Seoul National University, Seoul 08826, Korea

We observed efficient sub-Doppler cooling of ^{85}Rb atoms under a nonzero magnetic field in a moving optical lattice formed in a bichromatic magneto-optical trap. Trap laser detunings were biased or set differently for the counterpropagating laser beams so that the atoms could be trapped where the magnetic field was nonzero. We investigated the center position and the temperature of the atomic cloud. We found that the sub-Doppler cooling effect, known to decrease as the nonzero magnetic field increases in a magneto-optical trap, would in fact increase under a particular trap-laser detuning difference. We first derived the condition under theoretical considerations and then verified it experimentally by conducting nondestructive measurement of atomic temperature.

I. INTRODUCTION

The magneto-optical trap (MOT) is widely used to prepare cold neutral atoms and molecules at high density near the Doppler-limit temperature [1–3]. Those low-temperature neutral atoms are then used in various studies involved with Bose and Fermi quantum gas [4–6], cold atoms coupled with a high-Q cavity [7–9], Rydberg atom quantum information [10,11], etc. Moreover, the MOT itself is a nontrivial subject of study due to its complexity coming from anisotropic magnetic fields as well as continuous scattering of near-resonant laser light by trapped atoms. Recent studies include investigation of the dynamic properties [12–15] and the characteristics of resonant fluorescence [16–18] of the trapped atoms in MOTs.

Trapping and cooling of atoms under nonzero magnetic fields can be advantageous in some cases. The spin-flip of trapped atoms leading to atom loss can be suppressed under a nonzero magnetic field [19]. Moreover, if the magnetic field is nonzero, the target velocity in laser cooling will also be nonzero. By using this property, atoms can be transported spatially while maintaining a narrow velocity distribution [20–22]. However, if the magnitude of the magnetic field in an MOT increases, the sub-Doppler cooling effect is known to decrease [23–25]. As a result, atoms cannot be trapped in a well-confined space and thus it becomes difficult to control their scattering lengths and velocities. It would thus be useful to have a method to maintain the sub-Doppler cooling of the trapped atoms under a nonzero magnetic field in an MOT.

One way to load atoms in a region of nonzero magnetic field in an MOT would be to apply different laser detuning frequencies for the counterpropagating trap lasers. In this case, the optical pressures of each counterpropagating laser are different from each other. The optical pressure difference then induces the Doppler cooling to load atoms at a position with a nonzero magnetic field which can compensate for the detuning difference. Note this position is generally different from the resonant point of the sub-Doppler cooling. Therefore, as the laser detuning increases, the temperature of the atoms increases as the magnitude of the magnetic field increases at the center of the atomic cloud.

In the present study, we solve this problem by employing a moving optical lattice formed in a passively stabilized MOT [26] as a means of transporting the atomic cloud to a location where efficient sub-Doppler cooling can take place. As a result, we could achieve efficient sub-Doppler cooling of trapped atoms at around 30 μK under a nonzero magnetic field. From theoretical considerations, we first obtained the condition for maximizing the sub-Doppler cooling under a nonzero magnetic field and then verified it in experiments utilizing the moving optical lattice. The temperature of the atomic cloud was measured nondestructively with photon-counting heterodyne spectroscopy [27].

This paper is organized as follows. In Sec. II, we consider the effects of different frequency detunings of the counterpropagating lasers on atomic velocities in an optical molasses. Based on this consideration, we then discuss where the atoms are stably captured and where the sub-Doppler cooling is maximized in a moving optical lattice formed in a phase-stabilized bichromatic MOT. The experiment setup is described in Sec. III and the experimental results are presented in Sec. IV on the position and temperature of the atomic cloud. From these results we confirm the condition for maximizing the sub-Doppler cooling under a nonzero magnetic field. In Sec. V, we summarize our work and draw a conclusion.

II. THEORY

A. Trap location z_1 by one-photon transition for a large laser detuning difference

A major optical process occurring in an MOT is the one-photon transition of atoms induced by equally red-detuned

---

[*]Present address: Gajaeul Middle School, Seoul 03709, Korea.

[†]Present address: Samsung Electronics Company, Hwaseong 18448, Korea.
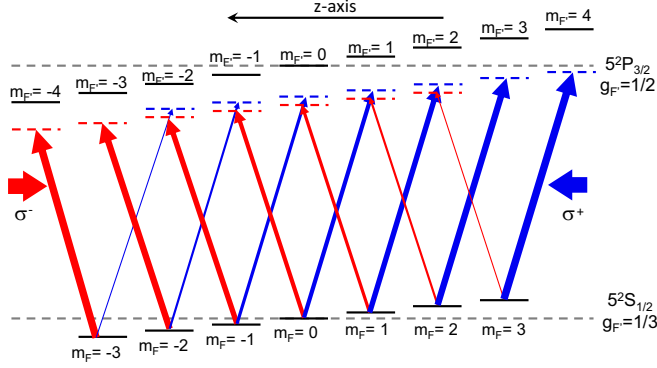
[‡]kwan@phya.snu.ac.kr

FIG. 1. One-photon transitions of ^{85}Rb atoms in the σ^+-σ^- polarization configuration with different detunings. The blue and red arrows indicate the transition of $\Delta m_F = \pm 1$, respectively, and the thickness of the arrows indicates the transition strength determined by the Clebsch-Gordan coefficients.

counterpropagating lasers. Suppose the red-detuned lasers are arranged in the σ^+-σ^- polarization configuration under an inhomogeneous magnetic field by an anti-Helmholtz coil. Although we deal with a three-dimensional (3D) MOT, we consider a one-dimensional (1D) MOT for simplicity since it has been shown that the trapping and damping forces in a 3D MOT with the energy level type considered in the present work are similar to those in a 1D MOT [28]. In this simplified arrangement, the atoms are trapped under the effect of Doppler cooling [19] at the location where the light pressures due to the one-photon transitions are balanced. The balancing occurs at the center of the anti-Helmholtz coil, where the magnetic field is zero.

If the frequencies of the counterpropagating lasers in the σ^+-σ^- configuration are set differently, the atoms can be trapped at a location where the magnetic field is nonzero and thus the light pressures due to the one-photon transitions are balanced. Note that under a nonzero magnetic field the magnetic sublevels of atoms are shifted by the Zeeman effect as shown in Fig. 1, where we consider rubidium-85 atoms. The resulting resonant frequency of the $5\,^2S_{1/2} \leftrightarrow 5\,^2P_{3/2}$ transition of ^{85}Rb is given by

$$\omega_{\text{shift}}(m_F, m_{F'}) = \omega_0 - \frac{g_F m_F \mu_B \beta z}{\hbar} + \frac{g_{F'} m_{F'} \mu_B \beta z}{\hbar}, \quad (1)$$

where ω_0 is the unshifted resonance frequency; $g_F(= 1/3)$ and $g_F'(= 1/2)$ are the Landé g factors of the lower and the upper sublevels, respectively; $m_F(m_{F'})$ is the magnetic quantum number of the lower(upper) sublevels; and β is the magnetic field gradient along the z direction. The resonance frequencies of the σ^+ and σ^- transitions with $\Delta m_F = m_F' - m_F = \pm 1$, respectively, are then given by

$$\omega_{\text{shift}}(\Delta m_F = \pm 1) = \omega_0 + \frac{[\pm g_{F'} - (g_F - g_F')m_F]\mu_B \beta z}{\hbar}. \quad (2)$$

The atoms in different sublevels experience unlike resonance frequencies with different transition strengths due to unequal Clebsch-Gordan coefficients for the σ^+ and σ^- transitions.

Let us assume that the σ^+ laser directed to the $+z$ direction has a larger frequency than the σ^- laser directed to the $-z$ direction as shown in Fig. 1 and their detuning difference $\delta\Delta$ is much smaller than the natural linewidth Γ of the transition: $\delta\Delta = \Delta_+ - \Delta_- \ll \Gamma$, where $\Delta_\pm = \omega_{\text{laser},\sigma^\pm} - \omega_0 < 0$, the detuning of the $\sigma^\pm$ trap laser, respectively. Consider then an atom in the $m_F = 3$ sublevel at $z > 0$. It is likely to absorb a photon from the σ^+ laser because the σ^+ transition has a Clebsch-Gordan coefficient larger than that of the σ^- transition. As a result, it will be pushed to $z' > z > 0$, where the magnetic field becomes larger. The increased magnetic field leads to more increased detuning for the σ^+ transition than for the σ^- transition, and therefore it is pushed back to a smaller $z'' < z'$ while m_F changes toward $m_F = 0$. Likewise, the atom in $m_F = -3$ will experience its m_F changing toward $m_F = 0$. Therefore, we expect that the $m_F = 0$ state will be most populated in an equilibrium.

In the $m_F = 0$ sublevel, for which the $\sigma^\pm$ transitions have the same Clebsch-Gordan coefficients, the light pressures by the counterpropagating lasers can be canceled out if the Zeeman shift difference can be compensated by the laser detuning difference:

$$\delta\Delta = \omega_{\text{shift}}(0, 1) - \omega_{\text{shift}}(0, -1) = \frac{2g_F' \mu_B \beta z}{\hbar}. \quad (3)$$

Therefore, the position z_1 where the optical pressure is balanced for a given detuning difference $\delta\Delta$ is then given by (with $g_F' = 1/2$)

$$z_1(\delta\Delta) = \frac{\hbar\delta\Delta}{\mu_B \beta}. \quad (4)$$

In the passively stabilized MOT that we consider below, for a small detuning difference $\delta\Delta \ll \omega_{\text{osc}}$, where ω_{osc} is the oscillation frequency of the optical lattice potential, the atoms tend to be localized at the minima of the moving optical lattice potential formed in the MOT, and therefore, the above consideration is not applicable. The speed of the moving optical lattice is given by $v = \delta\Delta/(2k)$, where k is the wave vector of the trap laser. As we increase $\delta\Delta$ so as to increase the speed of the optical lattice well beyond ω_{osc}/k, eventually atoms are no longer localized by the optical lattice and they move freely in the MOT. We thus expect that in this limit the atomic cloud will be formed close to the location given by Eq. (4).

It should be noted that the width of the atomic cloud is not proportional to $z_1(\Gamma)$ but rather to $\sqrt{z_1(\Gamma)}$. The rms MOT size Δz is given by $\Delta z = \sqrt{\langle z^2 \rangle} = \sqrt{\frac{k_B T}{\kappa}} = \sqrt{\frac{\hbar\Gamma}{2\kappa}(\frac{T}{T_D})}$ [29], where T_D is the Doppler temperature given by $T_D = \frac{\hbar\Gamma}{2k_B}(=144\,\mu\text{K}$ in our case) and κ is a function of the trap-laser detuning, the intensity, μ_B, and β. For $T = T_D$, we have $\Delta z = 26\,\mu\text{m}$ when the trap-laser intensity is twice the saturation intensity of the trap transition. This size is comparable to the observed position displacement z_1 in our experiment discussed in Secs. III and IV and thus it is not difficult to measure the center position z_1 of the atomic cloud in the experiment.

B. Location z_2 of efficient sub-Doppler cooling under a nonzero magnetic field

Sub-Doppler cooling can occur in an MOT via coherent multiphoton transitions between two ground-state m sublevels
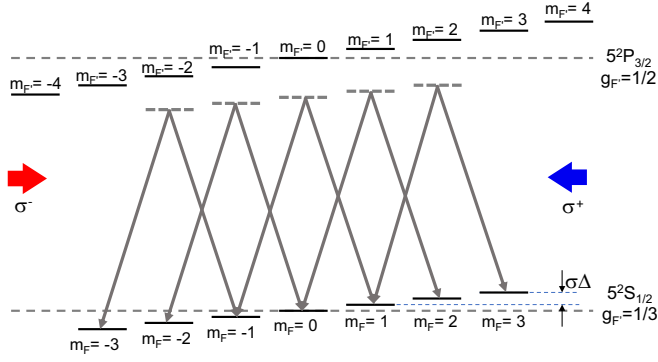
FIG. 2. Two-photon transitions of ^{85}Rb atoms in the σ^+-σ^- polarization configuration with different detunings under a nonzero magnetic field. When the Zeeman shift difference between the connected ground m sublevels is matched with the detuning difference of the trap lasers, the two-photon transition can occur resonantly, leading to sub-Doppler cooling of atoms to zero velocity.

[12,26,30,31] in the presence of spontaneous emission assisting energy dissipation [32]. Under the σ^+-σ^- configuration of the cooling lasers, atoms experience spatially rotating linear polarization. Consequently, depending on their motion, their m states change in such a way that an atom moving toward the $\sigma^+(\sigma^-)$ polarization laser experiences a coherent two-photon transition composed of coherent absorption of a $\sigma^+(\sigma^-)$ photon and simultaneous emission of a $\sigma^-(\sigma^+)$ photon. Thereby the atom experiences a $2\hbar k$-momentum kick in the opposite direction while the m_F value is decreased (increased) by 2. This cooling process continues until the atom stops.

In order for this two-photon transition to occur, the Zeeman shift difference of the connected ground m states should be exactly matched with the detuning difference $\delta\Delta$ as shown in Fig. 2. The condition for this is

$$\delta\Delta = \omega_{\text{shift}}(m_{F'} - 1, m_{F'}) - \omega_{\text{shift}}(m_{F'} + 1, m_{F'})$$
$$= \frac{2g_F\mu_B\beta z}{\hbar}. \tag{5}$$

Therefore, the location z_2 where the sub-Doppler cooling is maximized for a given trap-laser detuning difference $\delta\Delta$ is given by (with $g_F = 1/3$)

$$z_2(\delta\Delta) = \frac{3\hbar\delta\Delta}{2\mu_B\beta} = 1.5 \times z_1(\delta\Delta). \tag{6}$$

C. Accessing z_1 and z_2

In the passively stabilized MOT that we consider, a three-dimensional optical lattice is formed due to phase stabilization of six trap-laser beams. With different trap-laser frequencies, the optical lattice moves at a speed proportional to the frequency difference $\delta\Delta$. When $\delta\Delta \ll \omega_{\text{osc}}$, a large number of atoms are transported by the optical lattice while trapped at the local minima of the lattice potential until the atoms are no longer localized by the optical lattice near the edge of the MOT potential. As a result, the center position of the atomic cloud in the steady state tends to be much larger than z_1 and z_2. As we increase the trap-laser frequency difference further, more and more atoms are no longer trapped in the potential minima of the optical lattice. For a large frequency difference, $\delta\Delta \gg \omega_{\text{osc}}$,
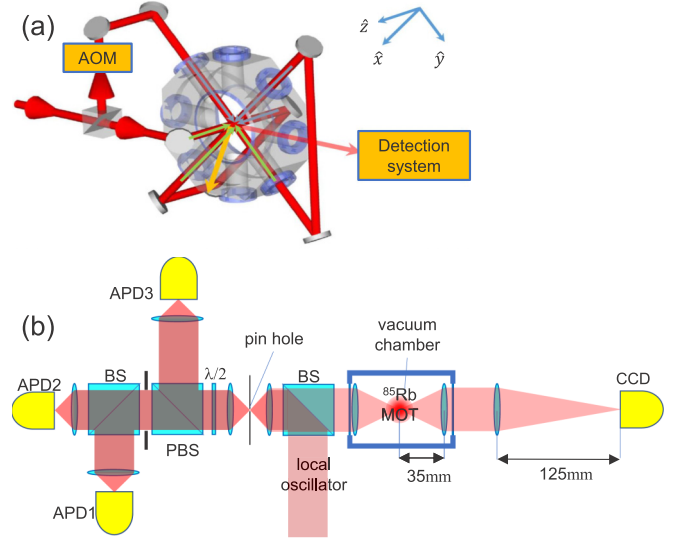

FIG. 3. (a) Configuration of the laser beams for a moving optical lattice in a passively stabilized MOT. (b) Schematic of the detection system. The heterodyne beat signal is measured on the left side with avalanche photodiode (APD) 1 and APD2, and the position of the atom is measured on the right side with a CCD. APD3 is used to align the pin hole.

the atoms can still be dragged to the moving direction of the optical lattice, resulting in a stable location of the atomic cloud away from the origin. We expect the cloud location would approach z_1 as $\delta\Delta$ is increased to a value well beyond ω_{osc}. Then for an intermediate frequency difference, the position of the atomic cloud would cross $z_2(> z_1)$, in the vicinity of which significant sub-Doppler cooling would then occur to lower the temperature of the atomic cloud. In the experiment discussed below, the position of the atomic cloud can thus be adjusted by the trap-laser parameters such as intensity and detuning without any other external forces.

III. EXPERIMENT

In our experiment, ^{85}Rb atoms were trapped by using an orthogonal three-way σ^+-σ^- optical arrangement with an anti-Helmholtz coil. In order to generate a stable optical lattice, we employed the passively stabilized beam configuration as shown in Fig. 3(a) [12,26]. In the axial direction (z direction) of the anti-Helmholtz coil, the magnetic field had a field gradient of $\beta = 240$ G/cm. The trap laser was red-detuned by $3\Gamma = 18$ MHz from the resonant frequency of the transition between the $5^2S_{1/2}$ $F = 3$ state and the $5^2P_{3/2}$ $F = 4$ state, and a repump laser was applied to the transition between the $5^2S_{1/2}$ $F = 2$ state and the $5^2P_{3/2}$ $F = 3$ state.

The optical lattice was made to move by introducing a frequency difference $\delta\Delta$ between counterpropagating trap-laser beams. It moved at a speed of $v = \delta\Delta/(2k)$ in the direction of the higher-frequency trap-laser beam. The frequency difference was varied from zero to 500 kHz with a 10-kHz interval. The frequency detuning of each trap-laser beam was adjusted by independent acousto-optic modulators (AOMs). The same AOMs were also used for power stabilization of the

passing trap-laser beams for accurate and stable position and spectrum measurements.

For a given set of the trap-laser intensity and the frequency difference, we performed the following measurements: atomic cloud images for the information on the atom position and the fluorescence spectrum for the information on the atom temperature. Toward this end, two objective lenses with a numerical aperture of 0.24 were mounted inside the vacuum chamber in opposite directions as shown in Fig. 3(b). They were separated from the MOT center by a focal length of 35 mm. In the coordinate system shown in Fig. 3(a), the optical lattice moves in the (1,1,1) direction and the objected lenses are directed in the $(-1,1,0)$ and $(1, -1,0)$ directions, and therefore the optical lattice moves in a common focal plane of the two objectives lenses allowing simultaneous measurement of the position and spectrum of the atoms.

An important feature of our experimental setup is non-destructive measurement. Note that the nonzero magnetic field and the light pressure at the location of the atomic cloud are inhomogeneous. This makes it difficult to apply the conventional time-of-flight technique to the measurement of the momentum distribution: it would be quite tricky to have the magnetic field and the optical pressure canceling each other during the entire turn-off time in the time-of-flight measurement. In our setup, instead, the momentum distribution is nondestructively obtained from the resonance fluorescence spectrum of the trapped atoms in the steady state. The spectrum is measured by using photon-counting-based second-order correlation spectroscopy (PCSOCS) [27]. In this technique, the resonant fluorescence is mode matched and mixed with a local oscillator whose frequency is shifted from that of the trap laser by 10 MHz, and then the second-order correlation of the resulting heterodyne beat note is measured. The Fourier transform of the second-order correlation then reveals the fluorescence spectrum of the atoms.

IV. RESULTS AND DISCUSSIONS

A. Position of the atomic cloud

The position displacement of the atom cloud measured as a function of the frequency difference $\delta\Delta$ is summarized in Fig. 4. In our magnetic field configuration, the restoring force in the x and y directions in Fig. 3 is smaller than that in the z direction because the magnetic field gradient in those directions is smaller than that in the z direction. For this reason, the atomic cloud is elongated in the x and y directions. In addition, the dragging of the atomic cloud by the moving optical lattice makes the cloud diffused toward the moving directions as the lattice speed is increased. For comparison with the theory in Sec. II B, we only considered the z displacement of the atomic cloud in Fig. 4.

It is seen that at small frequency differences the position of the atom cloud is shifted to a position larger than $z_2(\delta\Delta)$ as well as $z_1(\delta\Delta)$. This is the effect of the moving optical lattice: the atoms are continuously transported by the optical lattice to one side of the MOT. The distance from $z_2(\delta\Delta)$ is increased until $\delta\Delta \sim 100$ kHz, which is about the same as the oscillation frequency ω_{osc} associated with the local minima of the optical lattice potential. For $\delta\Delta \gg \omega_{osc}$, the
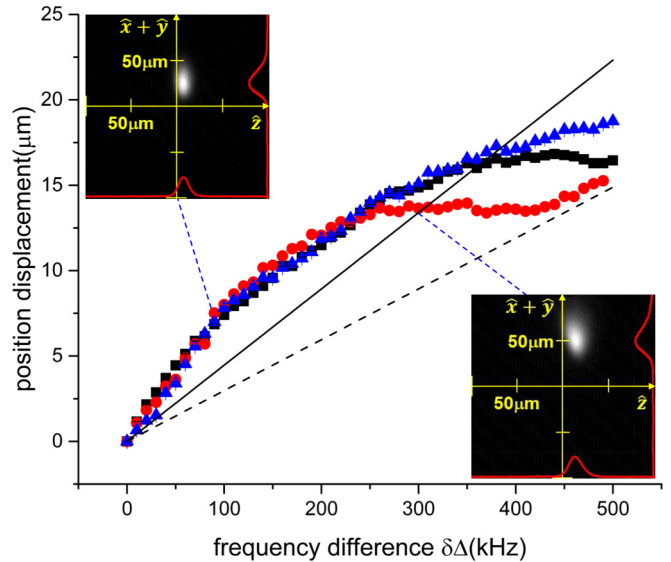

FIG. 4. Position displacement of the atom cloud as a function of the frequency difference $\delta\Delta$. The red circles are experimental results for $I/I_S = 0.67$, the black squares are for $I/I_S = 1.34$, and the blue triangles are for $I/I_S = 2.02$. The solid line indicates $z_2(\delta\Delta)$ and the dashed line $z_1(\delta\Delta)$. Experimental error, mostly due to the setup instability, is under 1 μm. In each image, the horizontal line corresponds to the z axis while the vertical line corresponds to the direction $\hat{x} + \hat{y}$ in Fig. 3. The red curves in each image represent the atom density distributions along the horizontal and vertical lines crossing the brightest point in the image.

atoms are no longer transported, while localized, by the optical lattice and thus the atom cloud position approaches $z_1(\delta\Delta)$, the equilibrium position by the one-photon transition. At an intermediate $\delta\Delta$, it crosses $z_2(\delta\Delta)$, the equilibrium position by the multiphoton transition. In Fig. 4, the results with three different trap-laser intensities, $I/I_S = 0.67$, 1.34, and 2.02, were compared, where I_S is the saturation intensity of the trap transition ($I_S = 3.8$ mW/cm^2). Note that the height of the optical lattice potential is proportional to the trap-laser intensity. It is seen that the higher the potential of the optical lattice the larger the frequency difference would be needed to get close to $z_1(\delta\Delta)$. All of these results are consistent with our theoretical expectations presented in Sec. II C.

B. Temperature of the atomic cloud

Since we are interested in the atoms not localized by the optical lattice, we pay attention to the results in the frequency region $\delta\Delta > 200$ kHz, where the population of unlocalized atoms (not localized by the optical lattice) becomes dominant. The atom temperature can be obtained from the fluorescence spectrum as shown in Fig. 5, which can be fit by five line-shape curves. The narrow central peak is the Rayleigh peak by the atoms localized in the optical lattice exhibiting the Lamb-Dicke narrowing [12,33]. It occurs at the frequency $\omega = \omega_0 + (\Delta_- + \Delta_+)/2$, which is the frequency of both counterpropagating trap lasers seen in the moving frame of the optical lattice. The small peaks on both sides close to the Rayleigh peak are Stoke and anti-Stoke Raman sidebands due to the oscillatory motion of the atoms trapped
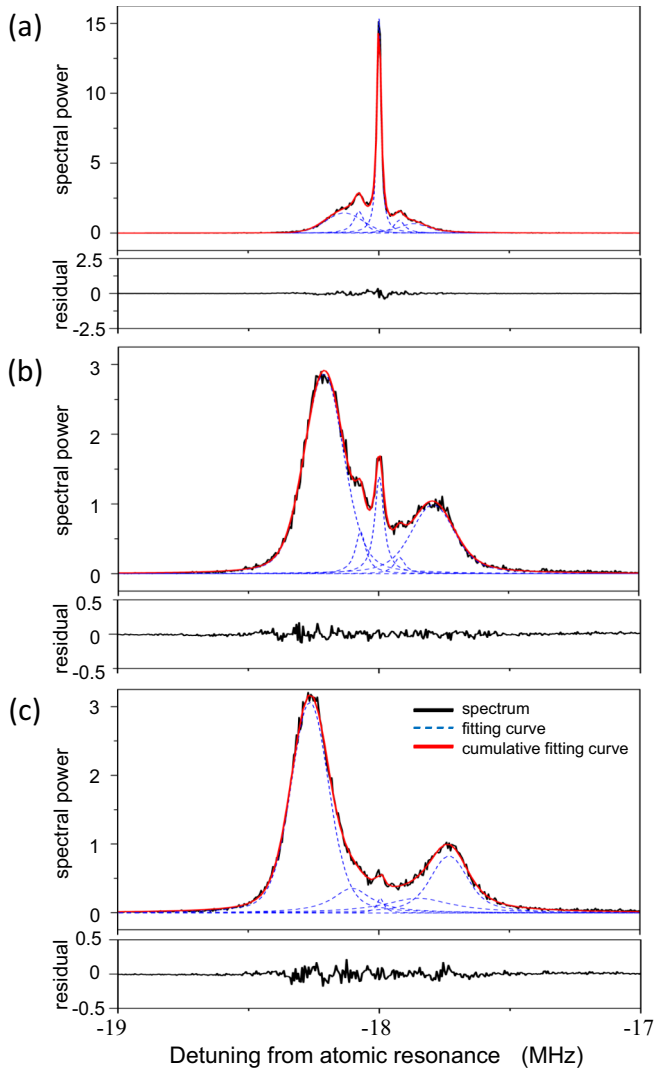
FIG. 5. The fluorescence spectra measured by using PCSOCS with (a) $\delta\Delta = 130$ kHz, (b) $\delta\Delta = 340$ kHz, and (c) $\delta\Delta = 460$ kHz. Black curves are the observed spectra. Blue dashed curves are fit curves while the red (gray) curves are the sum of the five fit curves. Outer broad peaks on both sides represent the momentum distribution of the atoms trapped but not localized in the optical lattice.

in the local minima of the optical lattice potential [12,26,31]. They are separated from the Rayleigh peak by the oscillation frequency ω_{osc}. The two broad and large peaks further away from the central peak are due to the unlocalized atoms, and they are centered around the trap-laser frequencies $\omega_0 + \Delta_-$ and $\omega_0 + \Delta_+$, exhibiting Doppler broadening, and thus separated from the Rayleigh peak by $\pm\delta\Delta/2$.

The peak heights of the nonlocalized atoms are different because the scattering rates of two counterpropagating lasers are different. As seen in Fig. 1, the effective detunings of the σ^+ and σ^- trap beams experienced by the atoms in various ground-state magnetic sublevels are different in a region of a nonzero magnetic field, and thus the scattering rates of the σ^+ and σ^- polarization lasers differ significantly. Moreover, the scattered light of the σ^+ trap beam is in an elliptical polarization different from that of the σ^- trap beam

while the detectors are measuring only the polarization in a particular direction (horizontal polarization in the laboratory coordinates), further deepening the discrepancy. A detailed analysis on the asymmetric peak heights is given in Ref. [34].

The area sum under the Rayleigh peak and the Raman sidebands is proportional to the probability of finding atoms localized in the optical lattice whereas the area sum under the
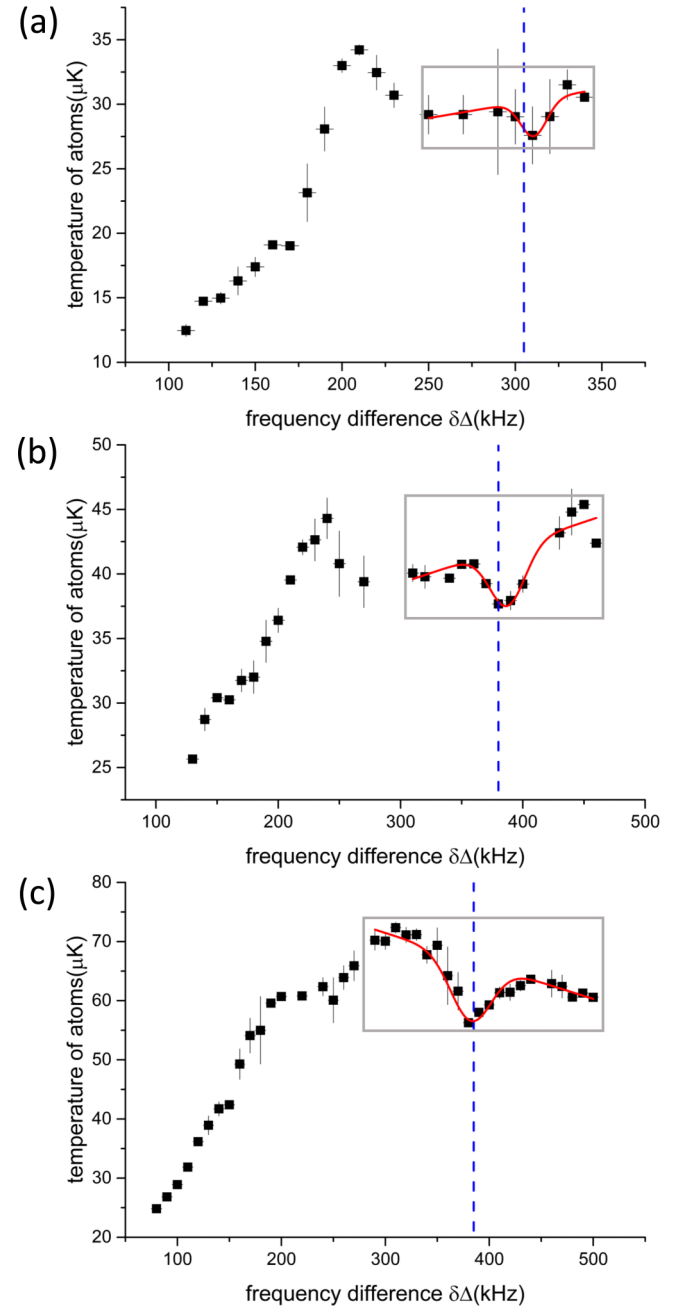

FIG. 6. The variation of the atom temperature with the frequency difference and the laser intensity. Black solid squares represent the temperature of atoms not localized in the optical lattice. The temperature decreases near the frequency difference that makes the atom cloud be located at z_2 in Fig. 4. This frequency is indicated by a blue vertical dashed line. Trap-laser intensities are as follows: (a) $I/I_S = 0.67$, (b) $I/I_S = 1.34$, and (c) $I/I_S = 2.02$. Red (gray) curves indicate a Gaussian fit with a tilted base line around the local minima in the range surrounded by a gray rectangle.

two broad peaks is proportional to the probability of finding atoms unlocalized in the optical lattice. The line shapes of the broad peaks represent Doppler broadening of the unlocalized atoms, giving us the information on the momentum distribution and thus the temperature of those atoms [12]. The line shapes can be fit by the Voigt profile, a convolution of a Lorentzian and a Gaussian. The Gaussian represents the inhomogeneous Doppler broadening of the thermal gas with the $1/e$ width equal to $\Delta \nu_D = \sqrt{\frac{2k_B T}{m\lambda^2}}$. Therefore, the temperature of the thermal gas can be obtained from the width of the Gaussian component. The resulting temperature of the thermal gas (unlocalized atoms) is plotted in Fig. 6.

Let us pay attention to Fig. 6(a), where it is seen that the temperature increases monotonically with the detuning frequency difference $\delta\Delta$ until $\delta\Delta$ reaches about 200 kHz. This frequency coincides with the point where the atomic cloud position starts to approach $z_1(\delta\Delta)$ and $z_2(\delta\Delta)$ in Fig. 4. The more atoms become unlocalized in the optical lattice as the frequency difference increases, the higher the temperature of those unlocalized atoms become. However, beyond 200 kHz, the temperature starts to decrease and then stays around 30 μK, much lower than $T_D(=140\,\mu\text{K})$, clearly indicating that significant sub-Doppler cooling must be taking place there. Moreover, the temperature shows a local minimum around 310 kHz. A similar trend is also observed in Figs. 6(b) and 6(c) with larger trap-laser intensities.

Comparing Figs. 4 and 6, we find that the sub-Doppler cooling is effective as long as the atom cloud position z_{atom} is in the vicinity of $z_2(\delta\Delta)$ or $|z_{\text{atom}} - z_2| \ll |z_{\text{atom}}|$. The vertical blue lines in Fig. 6 indicate the frequency difference corresponding to the multiphoton resonant position $z_2(\delta\Delta)$. Their positions are well matched with the local minima of the observed temperature determined by Gaussian fits in the aforementioned range of the frequency difference. These experimental results clearly support the validity of our formula, Eq. (6), presented in Sec. II B.

V. CONCLUSION

We investigated sub-Doppler cooling of ^{85}Rb atoms under a nonzero magnetic field in a moving optical lattice formed in a phase-stabilized bichromatic magneto-optical trap. There are two important optical processes when the detunings of the counterpropagating lasers are different. First, the light pressure due to one-photon transition is balanced at $z = z_1(\delta\Delta)$, where the Zeeman shift difference is matched with the frequency detuning difference $\delta\Delta$. Second, due to multiphoton transition, sub-Doppler cooling is maximized at $z = z_2(\delta\Delta)$. We found that the position $z_2(\delta\Delta)$ is 1.5 times larger than $z_1(\delta\Delta)$ and therefore it is impossible to achieve efficient sub-Doppler cooling in a conventional MOT under a nonzero magnetic field. In our experiment employing a phase-stabilized MOT with a moving optical lattice, however, we could load the atomic cloud at $z_2(\delta\Delta)$ by utilizing the dragging effect of the moving optical lattice formed in our MOT. We obtained the atomic cloud temperature by analyzing atomic resonance fluorescence spectra and measured the atom cloud position from their images in the trap. The temperature reached a local minimum around $z_2(\delta\Delta)$, where the most efficient sub-Doppler cooling occurred even in the presence of a nonzero magnetic field. The observed temperature varied from 30 to 60 μK, much lower than the Doppler temperature $T_D = 144$ μK of ^{85}Rb, as the trap-laser intensity was increased from $I/I_S = 0.67$ to $I/I_S = 2.0$. Our results provide a way of achieving efficient sub-Doppler cooling under a nonzero magnetic field in MOTs.

[1] E. B. Norrgard, D. J. McCarron, M. H. Steinecker, M. R. Tarbutt, and D. DeMille, Phys. Rev. Lett. **116**, 063004 (2016).

[2] J. P. McGilligan, P. F. Griffin, R. Elvin, S. J. Ingleby, E. Riis, and A. S. Arnold, Sci. Rep. **7**, 384 (2017).

[3] L. Anderegg, B. L. Augenbraun, E. Chae, B. Hemmerling, N. R. Hutzler, A. Ravi, A. Collopy, J. Ye, W. Ketterle, and J. M. Doyle, Phys. Rev. Lett. **119**, 103201 (2017).

[4] M. Lu, N. Q. Burdick, S. H. Youn, and B. L. Lev, Phys. Rev. Lett. **107**, 190401 (2011).

[5] B. Fröhlich, M. Feld, E. Vogt, M. Koschorreck, W. Zwerger, and M. Köhl, Phys. Rev. Lett. **106**, 105301 (2011).

[6] I. Bloch, J. Dalibard, and W. Zwerger, Rev. Mod. Phys. **80**, 885 (2008).

[7] K. Baumann, C. Guerlin, F. Brennecke, and T. Esslinger, Nature (London) **464**, 1301 (2010).

[8] Y. Choi, S. Kang, S. Lim, W. Kim, J.-R. Kim, J.-H. Lee, and K. An, Phys. Rev. Lett. **104**, 153601 (2010).

[9] A. Reiserer and G. Rempe, Rev. Mod. Phys. **87**, 1379 (2015).

[10] T. A. Johnson, E. Urban, T. Henage, L. Isenhower, D. D. Yavuz, T. G. Walker, and M. Saffman, Phys. Rev. Lett. **100**, 113003 (2008).

[11] M. Saffman, T. G. Walker, and K. Mø lmer, Rev. Mod. Phys. **82**, 2313 (2010).

[12] W. Kim, C. Park, J.-R. Kim, Y. Choi, S. Kang, S. Lim, Y.-L. Lee, J. Ihm, and K. An, Nano Lett. **11**, 729 (2011).

[13] G. Moon, M.-S. Heo, Y. Kim, H.-R. Noh, and W. Jhe, Phys. Rep. **698**, 1 (2017).

[14] O. Fedchenko, S. Chernov, A. McCulloch, M. Vielle-Grosjean, D. Comparat, and G. Schönhense, Appl. Phys. Lett. **111**, 021104 (2017).

[15] R. Romain, P. Verkerk, and D. Hennequin, Eur. Phys. J. D **67**, 211 (2013).

[16] Q. Baudouin, N. Mercadier, V. Guarrera, W. Guerin, and R. Kaiser, Nat. Phys. **9**, 357 (2013).

[17] W. Guerin, M. O. Araújo, and R. Kaiser, Phys. Rev. Lett. **116**, 083601 (2016).

[18] M. O. Araújo, I. Kresic, R. Kaiser, and W. Guerin, Phys. Rev. Lett. **117**, 073002 (2016).

[19] C. J. Foot, *Atomic Physics* (Oxford University, New York, 2005).

[20] A. Aspect, E. Arimondo, R. Kaiser, N. Vansteenkiste, and C. Cohen-Tannoudji, Phys. Rev. Lett. **61**, 826 (1988).

[21] S.-Q. Shang, B. Sheehy, P. van der Straten, and H. Metcalf, Phys. Rev. Lett. **65**, 317 (1990).

[22] R. Y. Ilenkov, A. V. Taichenachev, V. I. Yudin, and O. N. Prudnikov, J. Phys.: Conf. Series **951**, 012004 (2018).

[23] S. Chang and V. Minogin, Phys. Rep. **365**, 65 (2002).

[24] M. Walhout, J. Dalibard, S. L. Rolston, and W. D. Phillips, J. Opt. Soc. Am. B **9**, 1997 (1992).

[25] A. J. Berglund, S. A. Lee, and J. J. McClelland, Phys. Rev. A **76**, 053418 (2007).

[26] A. Rauschenbeutel, H. Schadwinkel, V. Gomer, and D. Meschede, Opt. Commun. **148**, 45 (1998).

[27] H.-G. Hong, W. Seo, M. Lee, W. Choi, J.-H. Lee, and K. An, Opt. Lett. **31**, 3182 (2006).

[28] J. Devlin and M. Tarbutt, New J. Phys. **18**, 123017 (2016).

[29] C. G. Townsend, N. H. Edwards, C. J. Cooper, K. P. Zetie, C. J. Foot, A. M. Steane, P. Szriftgiser, H. Perrin, and J. Dalibard, Phys. Rev. A **52**, 1423 (1995).

[30] S. Chang, T. Y. Kwon, H. S. Lee, and V. G. Minogin, Phys. Rev. A **64**, 013404 (2001).

[31] C. I. Westbrook, C. Jurczak, G. Birkl, B. Desruelle, W. D. Phillips, and A. Aspect, J. Mod. Opt. **44**, 1837 (1997).

[32] W. Ketterle and D. E. Pritchard, Phys. Rev. A **46**, 4051 (1992).

[33] H. T. Bookey, M. N. Shneider, and P. F. Barker, Phys. Rev. Lett. **99**, 133001 (2007).

[34] J.-R. Kim, Spectroscopic measurement of sub-Doppler cooling with two color σ^+-σ^- laser configuration, Ph.D. thesis, Seoul National University, 2017.